Sugar acid production on gold nanoparticles in slurry reactor

Worgul, Bernadette; Freites Aguilera, Adriana; Vergat-Lemercier, Camille; Eränen, Kari; Simakova, Olga; Held, Hendrik; Freund, Hannsjörg; Murzin, Dmitry; Salmi, Tapio

Published in:
Chemical Engineering Science

DOI:
10.1016/j.ces.2022.117948

Published: 12/10/2022

Document Version
Final published version

Chemical Engineering Science 260 (2022) 117948

Contents lists available at ScienceDirect

Chemical Engineering Science

journal homepage: www.elsevier.com/locate/ces

Sugar acid production on gold nanoparticles in slurry reactor: Kinetics, solubility and modelling

Bernadette Worgul [a,b], Adriana Freites Aguilera [a], Camille Vergat-Lemercier [a], Kari Eränen [a], Olga Simakova [a], Hendrik Held [b,c], Hannsjörg Freund [b,c], Dmitry Yu. Murzin [a], Tapio Salmi [a,*]

[a] Åbo Akademi University, Laboratory of Industrial Chemistry and Reaction Engineering (TKR), Turku/Åbo, Finland
[b] Friedrich-AlexanderUniversität Erlangen-Nürnberg (FAU), Institute of Chemical Reaction Engineering, Erlangen, Germany
[c] TU Dortmund University, Institute of Reaction Engineering and Catalysis, dortmund, Germany

HIGHLIGHTS

- Arabinose was successfully oxidized to arabinonic acid in a slurry reactor.
- Dispersed gold nanoparticles were used as catalyst.
- Oxygen solubility in the reaction solution was measured.
- Extensive kinetic study of the oxidation process was conducted, revealing the effect of oxygen pressure and pH.
- A kinetic model was developed and used to describe the experimental data.

ARTICLE INFO

Article history:
Received 2 February 2022
Received in revised form 5 May 2022
Accepted 20 July 2022
Available online 25 July 2022

Keywords:
Sugar
Sugar acid
Lactone
Gold catalyst
Oxygen solubility
Kinetics
Modelling
Semibatch reactor

ABSTRACT

Sugar acids obtained by oxidation of sugars are very valuable molecules which are used as chelating agents, binders as well as ingredients in pharmaceuticals. Arabinonic acid was prepared by oxidation of arabinose on gold nanoparticles deposited on an aluminium oxide carrier. A systematic reaction kinetic study was conducted to reveal the influence of oxygen partial pressure and pH on reaction rate and product selectivity. Experiments were carried out in a laboratory-scale semi-batch reactor which was operated at 70 °C and oxygen partial pressures 0.125–1.0 atm. The pH of the aqueous sugar solution was 6–8. Oxygen was continuously flowing through the semibatch slurry reactor and the pH was kept constant by adding NaOH during the experiments. The oxygen solubility in the reaction mixture was determined in separate experiments. A reaction mechanism was proposed for the formation of arabinonic acid (main product) and arabinolactone (intermediate by-product). The surface reaction of competitively adsorbed arabinose and oxygen was assumed to be rate determining for the arabinose consumption. For the formation of arabinonic acid from arabinolactone, the rate determining step was presumed to be the reaction between arabinolactone and sodium hydroxide. The reactor was described with the perfect backmixing model and the component mass balances were solved numerically during the estimation of kinetic parameters by nonlinear regression analysis. The kinetic model gives new insights in the reaction mechanism and described the experimental data very well. The model has potential for application in the oxidation of other monomeric sugars, too.

1. Introduction

Hemicelluloses appearing in large amounts in biomass, particularly in woody biomass are rich sources of sugar monomers and polymers. The names of common hemicelluloses reflect their chemical composition, for example, arabinogalactan, arabinoglucuronoxylan, galactogluco-mannan, glucomannan. By well-controlled hot water extraction, hemicelluloses can be separated from biomass, because the other dominating components in biomass, cellulose and lignin are practically insoluble in water at a neutral pH range (Murzin and Salmi, 2012, Luterbacher et al., 2014, Salmi et al., 2014, Mehtiö et al., 2016).

Arabinose is a monomeric sugar co-existing in ring and open forms in aqueous solutions. Arabinose monomers can be obtained in large amounts from the branched hemicellulose arabinogalactan

* Corresponding author.
E-mail address: tapio.salmi@abo.fi (T. Salmi).

https://doi.org/10.1016/j.ces.2022.117948
0009-2509/

Nomenclature

C	concentration
H	Henry's constant
h	salting-out parameter in Henry's constant
I	intensity
K	adsorption equilibrium constant
k	rate constant
m	mass
N	reaction route
n	amount of substance
p	partial pressure
Q	objective function
r	rate
t	time
V	volume
V'	volumetric flow rate
x	mole fraction
κ	Stern-Volmer constant
τ	decay time

Subscripts and superscripts

atm	atmospheric conditions
cat	catalyst
exp	experimental quantity
G	gas
i, j	component indices
t	time
TOT	total
0	reference state
*	surface property
[]	concentration

(AG) which appears in large amounts in the softwood species *Larix sibirica*. The hydrolysis of AG in the presence of homogeneous or heterogeneous acid catalysts yields a mixture of arabinose and galactose monomers (Kusema et al., 2011). A further chemical treatment of monomeric sugars is very exciting, because they can be isomerized, hydrogenated and oxidized to very valuable components, such as sugar alcohols and sugar acids. Heterogeneous catalysis plays a key role in these processes. Typical heterogeneous catalysts for sugar hydrogenation are nickel and ruthenium, whereas palladium and gold are used for sugar oxidation. In best cases, a complete sugar conversion and a very high yield (95–99 %) of the desired product is achieved.

Since the pioneering research of Haruta and Hutchings (Haruta, 1989, Hashmi and Hutchings, 2006) gold has been a subject of intensive research in oxidation catalysis (Thompson, 2006, Price et al., 2019). Gold nanoparticles are able to oxidize not only simple molecules such as carbon monoxide and alcohols, but also more complex organic molecules such as mono- and oligosaccharides. The research devoted to sugar oxidation has shown that gold is a better catalyst for sugar oxidation than palladium, which was previously the dominating catalyst for this process (Mirescu and Prüße, 2007, Murzina et al., 2008, Kusema et al., 2010, Simakova et al., 2011, Delidovich et al., 2013, Kusema and Murzin, 2013, Franz et al., 2021, Herrero Manzano et al., 2021). Palladium catalyst is however, prone to overoxidation and deactivation.

Especially arabinonic acid, the corresponding acid of arabinose, has many valuable applications, for instance as a sequestering agent, a binder, a corrosion inhibitor, a biodegradable chelating agent as well as an additive in pharmaceuticals and cosmetics. Furthermore, aldonic acids are promising substitutes to conventional monomers used in the production of synthetic polymers including polyesters and polyamides. The oxidation routes of arabinose in an aqueous environment are illustrated in Fig. 1: at high pH, the formation of the alkali salt of arabinonic acid is preferred, whereas low pH shifts the reaction route towards the formation of the arabinolactone intermediate. The figure indicates that it is very important to investigate the effect of pH and the oxygen concentration, since they are strong governing factors of the product distribution.

In catalytic three-phase processes, the gas solubility and gas-liquid mass transfer play a very decisive role in the process performance. Intensive mixing is used in kinetic investigations to suppress the gas-liquid and liquid-solid mass transfer resistances, but it is not self-evident that the partial pressure of the gas can directly be used in kinetic expressions instead of the real liquid-phase concentration of the dissolved gas. Therefore it is important to carry out separate gas solubility experiments in the reaction mixture. The solubility of oxygen in pure water and in glucose solutions have been reported previously (Wilhelm et al., 1977, Battino, 1981, Fogg and Gerrard, 1991, Tromans, 1998, van Stroe-Biezen et al., 1993, Dissolved Oxygen, 2019), but not in aqueous arabinose solutions in the presence of electrolytes.

In the current work, we have carried out systematic kinetic studies of arabinose oxidation on a Au/Al_2O_3 catalyst and determined oxygen solubility in arabinose solutions in the presence of electrolytes. The aim was to reveal the intrinsic reaction kinetics and to elucidate the reaction mechanism on gold nanoparticles dispersed on a support material. In previous research of our group (Da Silva Correia et al., 2019, Herrero Manzano et al., 2021) we have investigated the effect of temperature on the oxidation kinetics, and now the effort is focused on the influence of pH and oxygen partial pressure as well as gas solubility. A mathematical model based on surface reaction mechanisms for the oxidation kinetics will be presented and the model predictions will be compared with experimental data.

2. Experimental section

2.1. Oxygen solubility measurements

A well-stirred glass vessel equipped with a heating/cooling jacket was used in the measurement of oxygen solubility in aqueous sugar and sugar acid solutions. The aqueous solution was placed in the vessel which was vigorously stirred by a mechanical agitator. A mixture of oxygen and argon was continuously flowing through the liquid phase. All the measurements were carried out on-line: liquid temperature with thermocouples, pH with a pH meter and dissolved oxygen concentration with an optical sensor (PreSens OXYBase WR-RS485-L5). The operating principle of the sensor is based on the effect of dynamic luminescence quenching by molecular oxygen. The sensor consisted of a light source to illuminate the sensor (laser, light emitting diode, lamps), an optical fiber as signal transducer (plastic or glass fiber), a photodetector (photodiode, photomultiplier tube, CCD-array) and the optical sensor (indicator immobilized in a solid matrix). The oxygen concentration in the liquid is proportional to the luminescence intensity detected by the sensor. A schematic view of the measurement device is provided by Fig. 2.

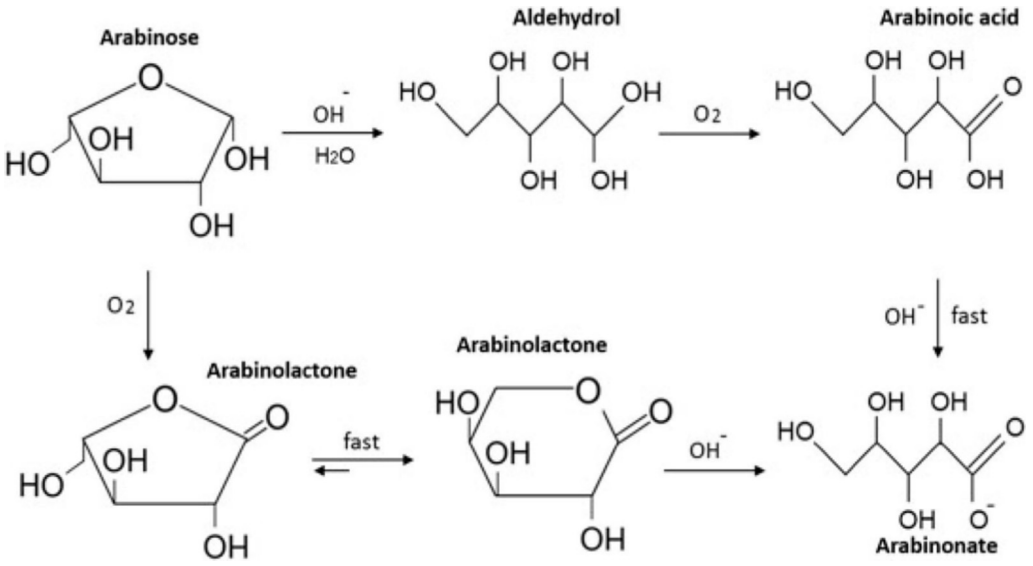

Fig. 1. Reaction routes in the oxidation of arabinose on gold (Da Silva Correia et al., 2019).

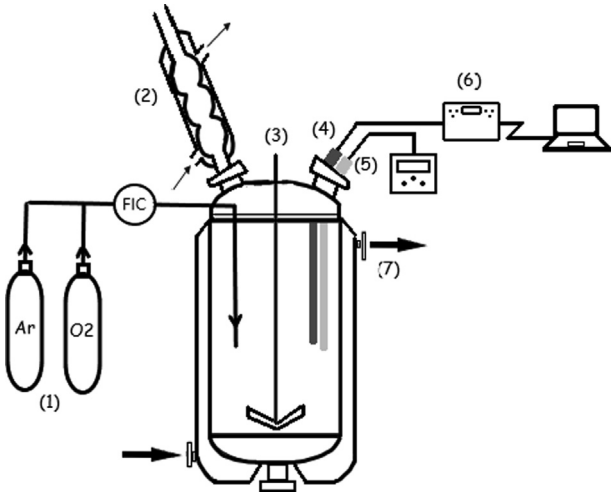

Fig. 2. Experimental device for the measurement of oxygen solubility. (1) gas supply, (2) cooler, (3) mechanical agitator, (4) oxygen sensor and thermometer (5) pH meter, (6) data acquisition system, (7) heating jacket.

To carry out the oxygen solubility measurements, the solution under study was placed in the glass vessel, the desired temperature was set on the heating/cooling thermostat and the mechanical agitator was set to 200 rpm. The gas was then introduced via a metal frit which injected it under the liquid surface. At the beginning of each experiment, the liquid phase was flushed with argon to ensure that the system was oxygen-free. After this, the oxygen flow was switched on.

2.2. Reactor system for oxidation experiments

All the experiments were carried out in an isothermal glass reactor (250 mL) equipped with an efficient gas entrainment impeller. The reactor vessel was heated by a heating jacket using water which was controlled by a Grant GD120 thermostat. Semi-batch operation mode was applied in the experiments. Oxygen was mixed with argon to ensure a suitable volumetric flow rate and to obtain the desired oxygen partial pressure. Both gas flows were controlled and adjusted using Brooks 5850S mass flow controllers. The gas was led through a metal frit to minimize the bubble size and to diminish mass transfer resistance due to oxygen diffusion into the liquid phase. The excess gas was vented via a cooler into atmosphere, thus preventing any vapors from escaping the reaction mixture. The pH and the temperature were measured with a Metrohm Titrando 907 unit equipped with a Metrohm Unitrode electrode. This device also controlled the pH of the liquid phase by adding a NaOH solution into the reaction mixture. Fig. 3 provides a schematic view of the reactor setup.

A laboratory-prepared Au/Al_2O_3 catalyst was used in a finely dispersed form, the particle size was <63 μm. The reaction temperature was 70 °C. Because the reaction is very sensitive for pH, and the pH tends to decrease during the reaction because of the sugar acid formation, a solution of NaOH was fed into the reactive liquid phase to maintain the pH constant during the experiments. The partial pressure of oxygen was varied between 0.125 and 1 atm, while the pH range of the experiments was 6–8.

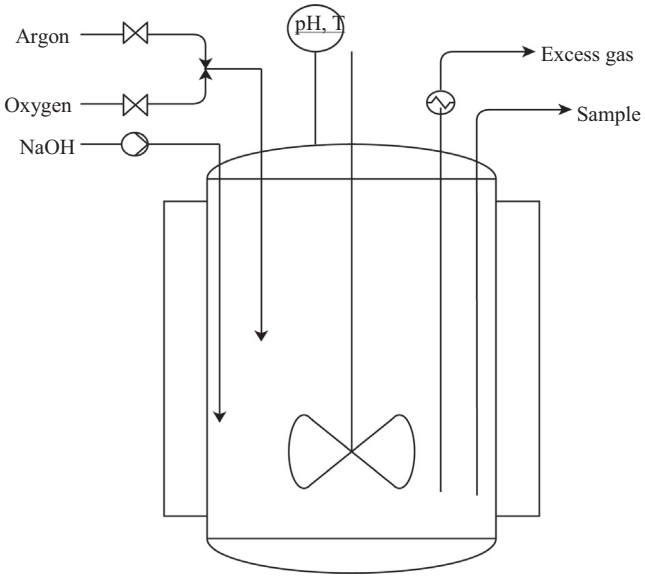

Fig. 3. Experimental set-up for sugar oxidation studies.

2.3. Experimental procedure in oxidation studies

An arabinose (Sigma-Aldrich; 99 wt%) solution with a volume of 125 mL was prepared and filled in the reactor vessel. After the solution had reached the desired temperature, the catalyst powder was added and the rest of the sugar solution was used to flush the inlet ensuring that all catalyst powder became immersed in the reaction mixture. The mechanical agitator was turned on and the pH control was started. The argon flow was kept on to maintain an inert atmosphere. As the temperature and pH had reached constant values, the first sample was withdrawn from the liquid phase and the argon flow was reduced or turned off while the oxygen flow was switched on. Table 1 displays the standard conditions chosen based on the previous experience of Franz et al. (2021) and Herrero Manzano et al. (2021).

During the experiments, several liquid samples were withdrawn with a syringe to follow the progress of the reaction. The sampling volume was 1 mL which was taken in two consecutive steps. First 0.3 mL were withdrawn and discarded to wash the sample tube, thereafter the final sample of 0.7 mL was taken. As the liquid-phase volume changed during the experiments due to added NaOH and withdrawing samples, it was important to take very exact sampling volumes and to track the feeding of NaOH.

After finishing the experiment, the reactor was filled with water and stirring was turned on for few minutes to clean the reactor. The reaction mixture was left to settle down and the sugar solution was carefully removed from the catalyst. The catalyst was then washed twice and dried before reuse.

The kinetic experiments were conducted under standard conditions with the exception of the varied experimental parameters (pH and oxygen partial pressure) and the mass of catalyst. To compare the experiments carried out with different masses of the catalyst, a normalized time (t_{norm}) was introduced. The measured time (t) was adjusted by the catalyst mass (m_{cat}) and the liquid volume (V): $t_{norm} = t\ m_{\mathrm{cat}}/V$. The total number of experiments was around 20, including preliminary experiments, repetitions and systematic experiments at various pH and oxygen pressure.

2.4. Chemical analysis

High performance liquid chromatography (HPLC) was used to identify the components and to determine their concentrations quantitatively. The samples withdrawn during the experiments were analysed with a HPLC (Hitachi Chromaster), which was equipped with a 300 × 7.8 mm Bio-Rad Aminex HPX-87C column and a refractive index detector (VWR Hitachi Chromaster). The analysis method of Franz et al. (2021) was implemented. To determine and quantify the components, the HPLC was calibrated with standard solutions thus allowing for a comparison of the retention times and the peak areas. The standard solutions consisted of different concentrations of arabinose, arabinolactone, arabinonic acid and ribulose in de-ionized water. The chemicals were calibrated separately and the retention times for the used components are shown in Table 2. Because the peaks in the chromatograms were not completely separated, the split-peak-method was used to determine the peak areas.

Table 1
Standard conditions used in kinetic experiments.

Parameter	Value	Unit
Temperature	70	°C
Arabinose concentration	0.133	mol/L
Oxygen partial pressure	0.125	atm
Gas volume flow	40	mL/min
Liquid volume	150	mL
pH	8	–
Stirring speed	980	rpm
Catalyst mass	0.1	g

2.5. Catalyst characterization

The catalyst was characterized with nitrogen adsorption by using a sorptometric instrument (Carlo Erba Sorptomatic) to obtain the specific surface area. Because the metal nanoparticle size is of crucial importance for the activity of gold catalyst, the gold nanoparticle size distribution was determined by high-resolution transmission electron microscopy (HR-TEM, JEM-1400Plus, JEOL Ltd.) The particle size distributions were calculated with the software ImageJ.

3. Oxygen solubility results

The results of the solubility measurements were interpreted with the Stern-Volmer equation, which describes the relationship between the oxygen concentration [O_2] in the solution, the luminescence intensity and its lifetime,

$$\frac{I_0}{I} = \frac{\tau_0}{\tau} = 1 + \kappa C_{O2} \tag{1}$$

where I and I_0 denote the luminescence intensities in the presence and in the absence of oxygen, respectively and τ and τ_0 are the corresponding luminescence decay times; κ is the Stern-Volmer constant. The solubility values obtained corresponded to a partial pressure of oxygen which in fact was lower than the atmospheric pressure since oxygen was in equilibrium with water vapor. Therefore, the oxygen concentration in the solution (C_{O2}) was corrected with the vapor pressure of water,

$$C_{O_2}(corrected) = C_{O_2}(exp)\frac{p_{atm}}{p_{atm} - p_w} \tag{2}$$

where p_{atm} and p_w denote the atmospheric pressure and water vapor pressure, respectively. In the literature (e.g. Fogg and Gerrard, 1991), the gas solubility is often expressed with Henry's law for sparingly soluble gases, which means that the concentration (mole fraction, x) of dissolved gas is directly proportional to the partial pressure,

$$x = \frac{p}{H} \tag{3}$$

where H is the Henry's constant and 1 atm is used as the reference pressure.

Oxygen solubility experiments were carried out at constant pH and temperature but varying the oxygen partial pressure (p_{O2}). For p_{O2}<1 atm, oxygen was mixed with argon (inert gas) to obtain the desired partial pressure of oxygen. The experimental results for pure water and two arabinose solutions are displayed in Fig. 4. The experiments confirmed the linear relationship (3) between the liquid-phase oxygen concentration and the partial pressure, which justifies the use of Henry's law for this case. Moreover, the dependence of the oxygen solubility on the arabinose concentration was non-significant.

Table 2
Retention times of calibrated reactants and components in HPLC.

Component	Retention time [min]
Arabinose	13.2–13.75
Arabinonic acid	16.1–17.6
Arabinolactone	10.8–11.7
Ribulose	19.5–20.3

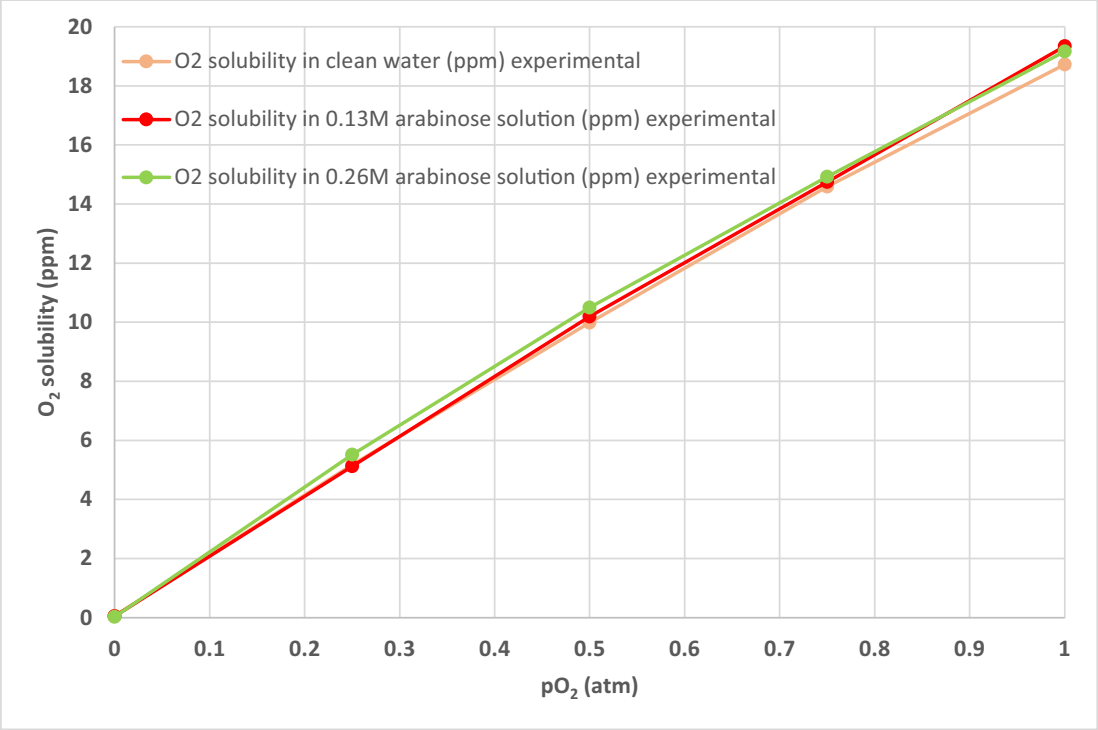

Fig. 4. Confirmation of the Henry's law for oxygen solubility in pure water and aqueous arabinose solutions.

The presence of electrolytes decreases the solubility because of the salting-out effect. Weisenberger and Schumpe (1996) have proposed a correction factor for the Henry's constant (H),

$$lnH = lnH_0 + \Sigma(h_i + h_G)C_i \quad (4)$$

where h_i and h_G are the salting-out parameters of the ion (i, i = Na^+, i = OH^- in this case) and the gas (g), C_i is the ion concentration and H_0 is the Henry's constant for a pure solvent.

since kinetic experiments were conducted at various pH-values, the oxygen solubility was measured within the same pH range by adding few droplets of HCl (0.02 mol/L) and NaOH (0.02 mol/L) to the aqueous solutions. The results given in Supplementary material indicate that the solubility was independent of pH, i.e. the ion concentrations under the actual experimental conditions; thus the salting out effect in equation (4) can be discarded for our investigations.

The coupled effect of pH and sugar concentration was studied with experiments carried out at two different arabinose concentrations at the pH range 6–8. The results shown in Supplementary material indicate that the effect of both the arabinose concentration and pH is in practice non-existent in this case.

Finally an issue is worth commenting: the sugar molecule is converted to the sugar acid during the course of the reaction – does this shift in the chemical composition affect the oxygen solubility? Arabinonic acid was not available in sufficiently large quantities; therefore some indicative experiments were carried out with different gluconic acid concentrations (see Supplementary material). A slight increase of the oxygen solubility (1–4 %) was noticed in the presence of the gluconic acid; however at the reaction temperature (70 °C) the increase was 1 % or even less. This increase might be explained by the interaction of dissolved oxygen and the carboxyl group of gluconic acid. A similar minor effect is likely to occur for arabinonic acid, too.

4. Catalyst characterization and activity testing results

The catalyst was analysed with high-resolution electron microscopy (HR-TEM). The gold nanoparticle particle size distribution was the catalytically active range reported for gold (<5 nm) (Simakova et al., 2011, Franz et al., 2021). An example of the nanoparticle size distribution is shown in Fig. 5. The oxidation

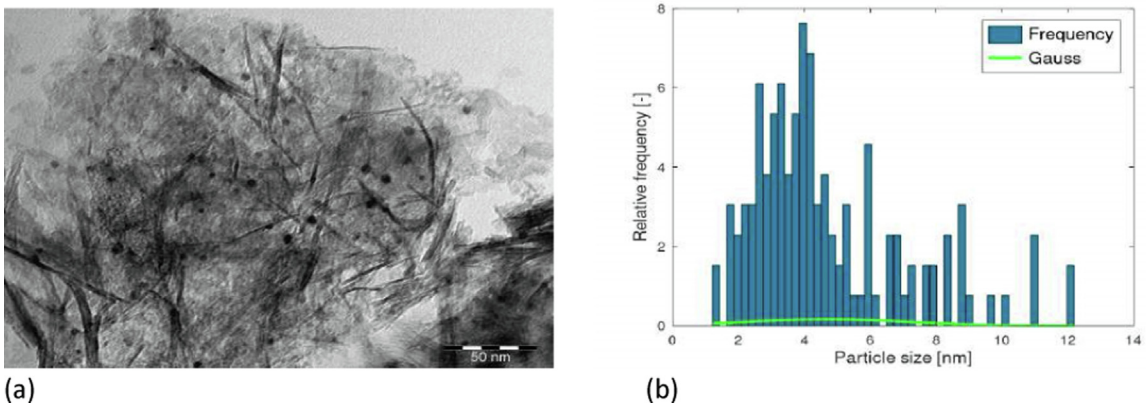

Fig. 5. HR-TEM image (a) and gold nanoparticle size distributions (PSD) of the catalyst (b).

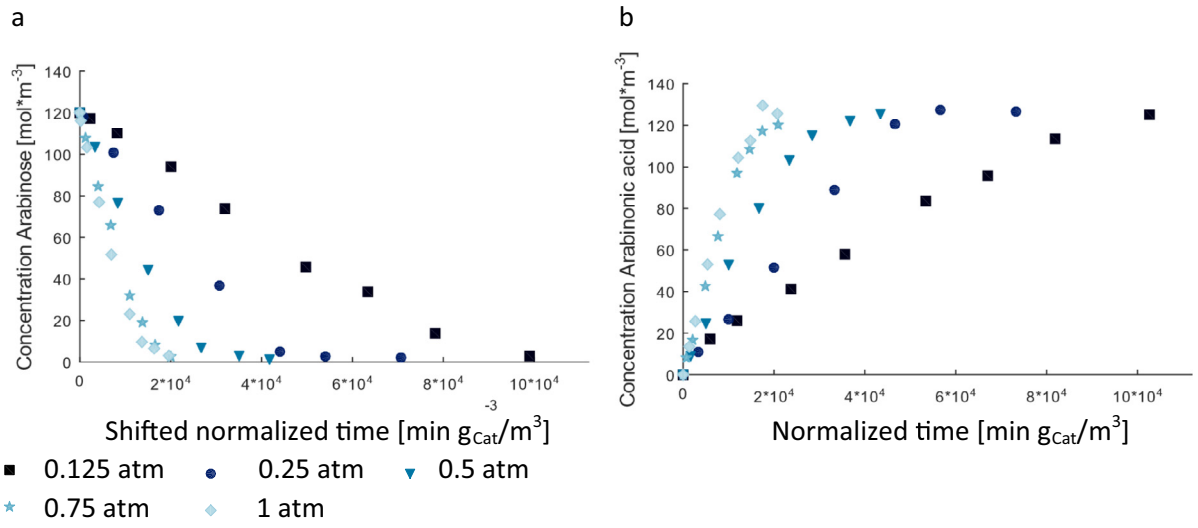

Fig. 6. Influence of oxygen partial pressure on catalytic results. T = 70 °C, pH = 8, $c_{Arabinose,0}$ = 133 mol/m^3, V' = 40 mL/min, stirring rate = 980 rpm. Concentrations of arabinose (a) and arabinonic acid (b).

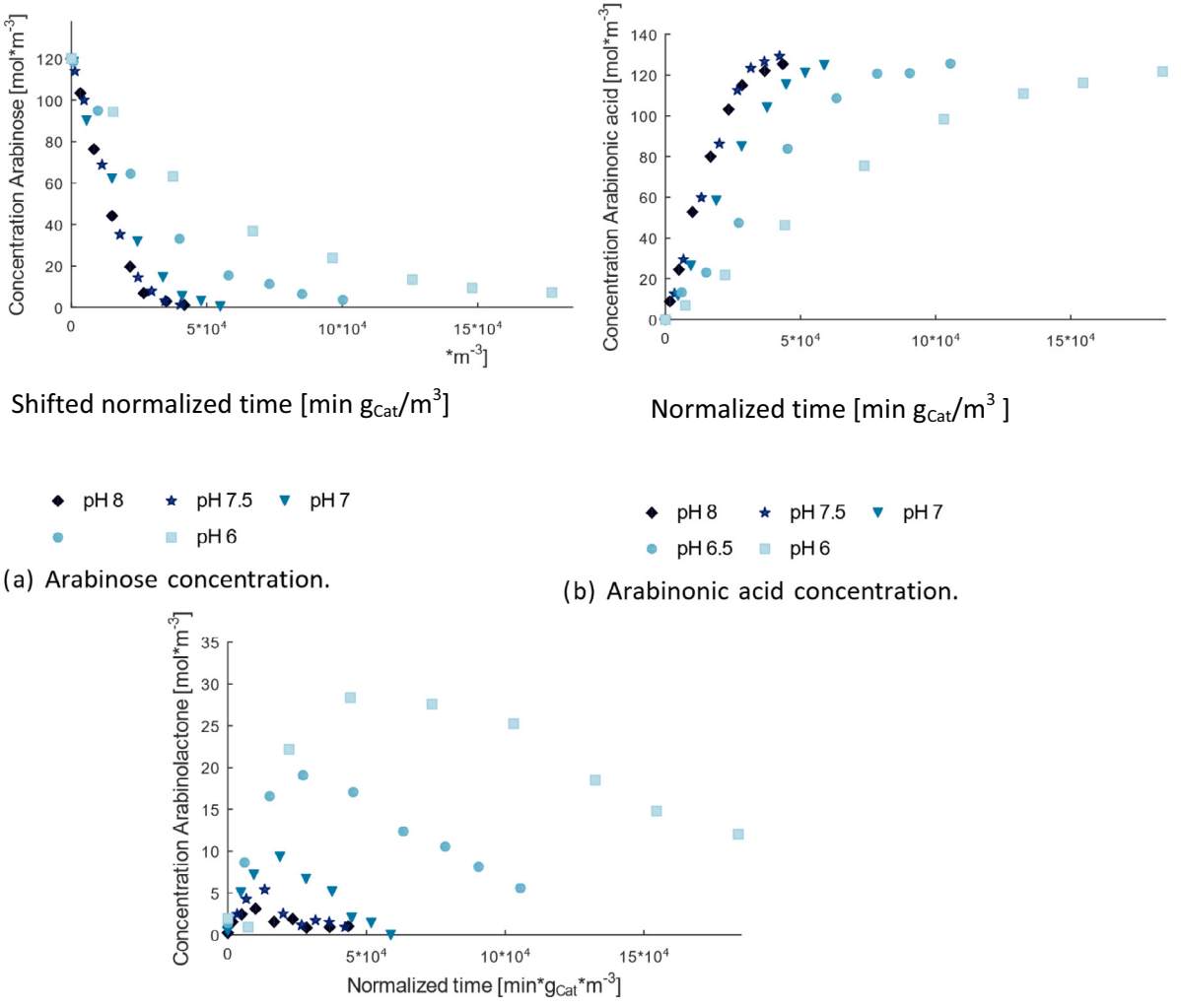

Fig. 7. Influence of pH on catalyst 4. T = 70 °C, pH = 8, $c_{Arabinose,0}$ = 133 mol/m^3, V' = 40 mL/min, oxygen partial pressure 0.5 atm, stirring rate = 980 rpm.

state of gold is an issue. This catalyst has been investigated previously by Simakova et al. (2011) by applying X-ray photoelectron spectroscopy (XPS) and the dominant form of gold has been confirmed to be metallic (Au^0).

5. Results of kinetic experiments

5.1. Influence of oxygen partial pressure on reaction kinetics

The results of the kinetic experiments at different oxygen partial pressures are shown in Fig. 6. The time scale was shifted for all experiments to start at an arabinose concentration of 120 mol/m^3. Hence, a shifted normalized time (t_{shift}) was introduced: the normalized time zero (0) corresponded to the arabinose concentration 120 mol/m^3 in each experiment. To calculate the shift in time (Δt) from the normalized time, linear interpolation of the first two experimental data points (t_0,c_0 and t_1,c_1) is used: the shift time is thus obtained from the equation Δt = (120 mol/m^3 - c_0)t_1/(c_1 – c_0). An increase in the oxygen partial pressure resulted in an expected increase in the reaction rate due to the increase of the oxygen concentration in the liquid phase. At lower oxygen partial pressures, this increase was more pronounced while a change from 0.75 atm to 1 atm barely exhibits any change reflecting the complete coverage of available sites at such conditions.

5.2. Influence of pH on reaction kinetics

Significant changes in the reaction rate could only be observed at pH values below 7. A change from pH 8 to pH 7.5 had nearly no effect on the consumption of arabinose or the formation of arabinonic acid and a further decrease to pH 7 showed only a slightly slower reaction. On the other hand, entering an acidic environment led to a significant decrease in the reaction rate and a profound increase in the concentration of arabinolactone was observable. Fig. 7 provides detailed information on the product distribution.

A change in pH corresponds to a change in the concentration of hydroxide ions (OH^-). As shown by Fig. 1, the oxidation reaction mainly consists of two steps: first the reaction of arabinose and oxygen to arabinolactone and the reaction of arabinolactone and water to arabinonic acid. The latter reaction is catalysed by OH^- ions. The decrease of the OH^- concentration clearly hinders the consumption of arabinolactone thus retarding the formation of arabinonic acid and increasing the arabinolactone concentration in the reaction mixture. Furthermore, the second reaction takes place in the liquid phase, while the first reaction takes place on the catalyst surface. Hence, arabinolactone needs to desorb in order to react with water. As adsorption and desorption are reversible processes, they depend on the concentration of the component. High concentrations shift the equilibrium towards adsorption thus high concentrations of arabinolactone in the liquid phase keep more active sites on the catalyst occupied. This leaves less vacant sites available for the adsorption of oxygen and arabinose, which retards the reaction rate. Moreover, Kusema et al. (2010) have proved a strong adsorption of arabinonic acid onto the catalyst at low pH values, hence more adsorption sites are blocked, which reduces the activity further.

The amount of available oxygen was verified to guarantee that the reaction is not limited by an insufficient amount of oxygen available in the liquid phase. Depending on the oxygen partial pressure, the oxygen flow was calculated assuming that the whole 250 mL reactor was filled. The values for the different oxygen flows and the average reaction rates for each experiment based on the experimental data are compared in Table 3. The calculated values confirm that the oxygen flow was at least two times larger than the reaction rate proving no limitations due to the oxygen flow. Thus the concentration of oxygen in the liquid was assumed to remain constant at the saturation level during the course of the experiment. The reaction rates for the variation of the pH are not shown in detail as the oxygen flow was kept constant and the reaction rates were equal or lower compared to the reaction rate at pH 8.

Table 3
Comparison of oxygen flow rates and reaction rates in dependence of the oxygen partial pressure at pH 8.

Partial pressure i [atm]	Oxygen flow rate [mol/(L min]	Reaction rate [mol/L min]	Flow: Reaction rate –
0.125	1.66 10^{-3}	0.78 10^{-3}	2.13
0.25	3.33 10^{-3}	1.63 10^{-3}	2.04
0.5	6.65 10^{-3}	1.24 10^{-3}	5.35
0.75	9.98 10^{-3}	1.08 10^{-3}	9.28
1	13.30 10^{-3}	1.50 10^{-3}	8.86

The Weisz-Prater criterion (Weisz and Hicks, 1962) showed very convincingly that the impact of internal diffusion resistance in the catalyst particles on the kinetics was negligible. Moreover, high stirring rates (980 rpm) were used removed the external mass transfer limitations. In this sense, this work is very analogous with our previous publication (Herrero Manzano et al., 2021).

6. Reaction kinetic modelling of arabinose oxidation

6.1. Reaction mechanism

To describe quantitatively the oxidation behavior of arabinose a well-structured model has been proposed by Da Silva Correia et al. (2019), partially based on a model previously developed by Kusema et al. (2012). The model considers the oxidation of cyclic arabinose taking both reaction routes via arabinolactone and aldehydrol into account. Hence, this model is used as a basis for describing the dependence of the reaction rate on pH and oxygen partial pressure. In our experiments, no aldehydrol was observed (Fig. 1); therefore a simplified scheme was adopted, comprising the formation of arabinolactone and conversion of it to arabinonic acid or arabinonate. The nomenclature and the reaction routes (N^I, N^{II}) and presumed elementary steps for the oxidation are listed in Tables 4-5.

Reaction routes N^I and N^{II} consider the oxidation of cyclic arabinose, To oxidize the cyclic form of arabinose, arabinose and oxygen are adsorbed (step 1 and 2) on the catalyst surface and react to form OOH $*$ and monodehydrogenated arabinose (step 3). These two species quickly react to form arabinolactone and hydrogen peroxide (H_2O_2) (step 4). In the next step, arabinolactone desorbs from the catalyst (step 5) and is hydrolyzed to form arabinonic acid (step 6). This reaction is catalyzed by hydroxide ions which also lead to a rapid neutralization of the arabinonic acid formed (step 7).

All adsorption and desorption steps are considered to reach an equilibrium rapidly thus they are not significantly influencing the overall reaction rates. In this work, the reaction route via the acyclic arabinose is neglected as the amount of acyclic arabinose is very

Table 4
Nomenclature of reaction network.

Active site	*
Arabinose	Ara
Arabinolactone	AraL
Arabinonic acid	AraA
Arabinonate	$AraA^-$

Table 5
Reaction steps and routes.

	N^{I}	N^{II}
1 $Ara + * \leftrightarrow Ara*$	1	0
2 $O_2 + * \leftrightarrow O_2*$	1	0
3 $Ara + O_2* \rightarrow RCO* + OOH*$	1	0
4 $RCO* + OOH* \overset{fast}{\rightarrow} AraL* + H_2O_2 + *$	1	0
5 $AraL* \leftrightarrow AraL + *$	1	0
6 $AraL + H_2O \overset{OH^-}{\rightarrow} AraA$	0	1
7 $AraA + OH^- \overset{fast}{\rightarrow} AraA^- + H_2O$	0	1

small compared to cyclic arabinose (Da Silva Correia et al., 2019) and no aldehydrol was detected as an intermediate. The isomerization of arabinose to ribulose was neglected, because the amounts of ribulose found in the HPLC analysis were insignificant. Hence, only the reaction routes N^{I} and N^{II} were taken into account in the final kinetic modelling. Because of the elevated temperature, hydrogen peroxide could not be detected, but it was decomposed to water and oxygen. Based on this reasoning, a simplified kinetic model can be derived for the system. Based on previous investigations of gold catalysts, the adsorption of oxygen was presumed to be molecular, because gold is not able to dissociate oxygen (Behravesh et al., 2020).

6.2. Model equations

For arabinose oxidation, the surface reaction rate can be expressed as.

$$r_1 = k_1 c_{ARA} * c_{O2}* \tag{5}$$

The reaction of arabinolactone takes place between adsorbed lactone and hydroxide ions in the solution, thus the rate equation becomes.

$$r_2 = k_2 c_{ARAL} * c_{OH} \tag{6}$$

The hypothesis of adsorption quasi-equilibria of the participating molecules implies that.

$$K_i = \frac{c_i*}{c_i c*} \tag{7}$$

The total balance of active sites is written with the aid of adsorbed species (c^*_j) and vacant surface sites (c^*),

$$c* + \sum c_j* = c_{TOT} \tag{8}$$

where c_{TOT} denotes the total concentration of available sites on the catalyst surface. Taking into account the quasi-equilibrium equilibria, the concentration of vacant sites is obtained from the total site balance,

$$c* = \frac{c_{TOT}}{1 + \sum K_j c_j} \tag{9}$$

Analogously, for each adsorbed molecule is valid.

$$c_i* = \frac{K_i c_i c_{TOT}}{1 + \sum K_j c_j}$$

After inserting equation (9) in the rate equations (5)-(6) and taking into account the adsorption quasi-equilibria (7), the following expressions are obtained for the reaction rates,

$$r_1 = \frac{k_1' c_{ARA} c_{O_2}}{(1 + \sum K_j c_j)^2} \tag{10}$$

$$r_2 = \frac{k_2' c_{ARAL} c_{OH}}{1 + \sum K_j c_j} \tag{11}$$

where the composite kinetic parameters are defined as.

$$k_1' = k_1 K_{ARA} K_{O_2} c_{TOT}^2 \tag{12}$$

$$k_2' = k_2 K_{ARAL} c_{TOT} \tag{13}$$

The adsorption term is.

$$\sum K_j c_j = K_{ARA} c_{ARA} + K_{ARAL} c_{ARAL} + K_{O_2} c_{O_2} \tag{14}$$

If the reaction of lactone is assumed to be homogeneous liquid-phase reaction, the denominator in r_2, Eq. (11) is 1. The generation rates of the components are obtained in a straightforward way from the stoichiometry,

$$r_{ARA} = -r_1 \tag{15}$$

$$r_{ARAL} = r_1 - r_2 \tag{16}$$

$$r_{ARAA} = r_2 \tag{17}$$

$$r_{O2} = -0.5 r_1 \tag{18}$$

$$r_{OH} = -r_2 \tag{19}$$

The material balances of the components in the molar form are expressed with the pseudo-homogeneous model for the system,

$$\frac{dn_i}{dt} = r_i m_{CAT} \tag{20}$$

The concentrations needed in the rate equations are obtained from the amounts of substance and the volume,

$$c_i = \frac{n_i}{V} \tag{21}$$

The liquid volume was changing during the reaction because a NaOH solution was added with a varying flow rate V' and the samples with volumes V_S were withdrawn,

$$V = V_0 + \int V' dt - \sum V_S \tag{22}$$

The mass balance for oxygen is excluded as oxygen is continuously fed into the reactor and thus the concentration of dissolved oxygen in the liquid phase remained constant at the saturation level.

Finally the model was solved numerically with the backward difference method implemented in the software Julia (White, 2020). The optimization problem was solved by minimizing the objective function (Q) with a Levenberg-Marquardt algorithm using the full time interval of each experiment,

$$Q = \sum_i \sum_t (c_{i,t\,\mathrm{exp}} - c_{i,t})^2 \tag{23}$$

where the index 'exp' refers to the experimental observation and $c_{i,t}$ is the concentration value predicted by the model for the respective

Table 6
Kinetic and adsorption parameters estimated for varying the oxygen partial pressure.

Parameter	Value	Error/%
k_1	53.99	9
K_{ARA}	0.01826	7
K_O	0.2411	54

Correlation matrix

	k_1	K_{ARA}	K_O
k_1	1.0	0.778	0.648
K_{ARA}	0.778	1.0	0.148
K_O	0.648	0.148	1.0

Units: k_1 = () mol min^{-1} kg^{-1} $(mol/m^3)^{-2}$, K_{ARA}, K_O = () $(mol/m^3)^{-1}$.

species (i.e. arabinose, arabinolactose, arabinonic acid). In order to improve the fit of the model, the second sample withdrawn was used as the starting point for each experiment.

6.3. Modelling results: Change of oxygen partial pressure

By varying the oxygen partial pressure only marginal amounts of arabinolactone below 3 mol/m^3 were detected presuming the reaction route N^{II} to be very rapid. Thus the combination of the reaction routes N^{I} and N^{II}, was considered, and $r_2 = 0$. The values of kinetic and adsorption constants obtained by implementing the model along with their errors are shown in Table 6 while the calculated concentration profiles are displayed in Fig. 8. The predicted concentration profiles clearly illustrate a good accordance between calculated and experimental data. The correlation matrix of the parameters is displayed in Table 6. The highest value of the correlation coefficients is 0.778 thus the statistic reliability of the estimated parameters can be regarded as satisfactory.

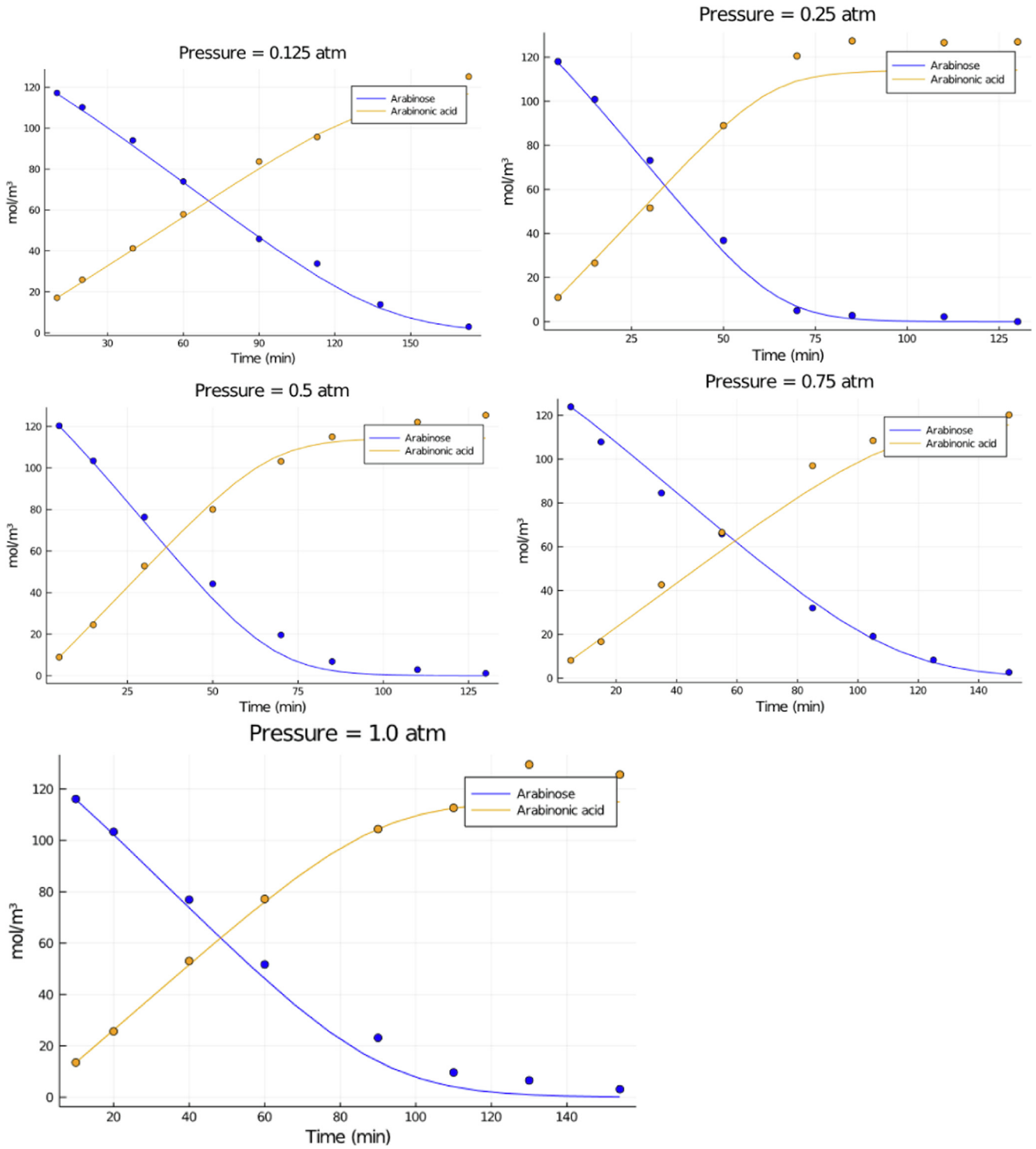

Fig. 8. Experimental (dots) and calculated (lines) concentration profiles for variation of the oxygen partial pressure at standard conditions (Table 1).

Parity plots describe the relation between all the experimental concentrations and concentrations predicted by the kinetic model. In the ideal case, the parity plot is a straight line with the slope 1, i.e. a complete coincidence between the experiments and the model. To further investigate the adequacy of the model a parity plot was made using all concentrations (Fig. 9). Only small deviations, mostly below 10 % over the investigated concentration range, are visible, thus confirming the reliability of the model.

6.4. Modelling results: Influence of pH

The complete kinetic model was used for this case, because the pH influences both reaction routes, N^{I} and N^{II}, and higher concentrations of arabinolactone (up to 30 mol/m^3) were detected in the experiments. Again the material balances were again expressed in molar form using by the pseudo-homogeneous model. For the hydroxide ions, the balance was set to zero, because NaOH was constantly added to keep the pH and hence the concentration of hydroxide ions was constant during the reaction. Furthermore, the adsorption constant for oxygen was fixed to the value determined by the change of the oxygen partial pressure as the correlation with the other parameters became otherwise too high making the estimation unreliable.

The results for the kinetic parameters along with the correlation matrix are shown in Table 7 and the concentration profiles are displayed in Fig. 10. A good fit of the calculated data to the experimental was obtained, which was also confirmed by the parity plot in Fig. 11. Only for pH 6, larger deviations can be observed as the calculated concentration profiles predict a faster consumption of arabinose and arabinolactone. A reason could be further additional effects, such as weaker adsorption of arabinonic acid in the acidic environment, which hampers the reaction. Such a pH dependent adsorption coefficient influencing also the lumped kinetic constant k_1' was not considered in the model. If the reaction of lactone (r_2) was considered as a homogeneous liquid-phase reaction and the denominator in equation (11) was set to 1, a very similar fit of the model was obtained, so this issue cannot be solved by data fitting.

6.5. Discussion of the experimental and modelling results

The main novelty of this work is the systematic investigation of the oxygen pressure and pH effects on sugar oxidation. Fig. 10 demonstrates the very clearly the enhancement of the reaction as the oxygen pressure is increased: for the partial pressure 0.25 atm, high conversion of arabinose (<95 %) is reached within 90 min, whereas 160 min is required to reach the high conversion

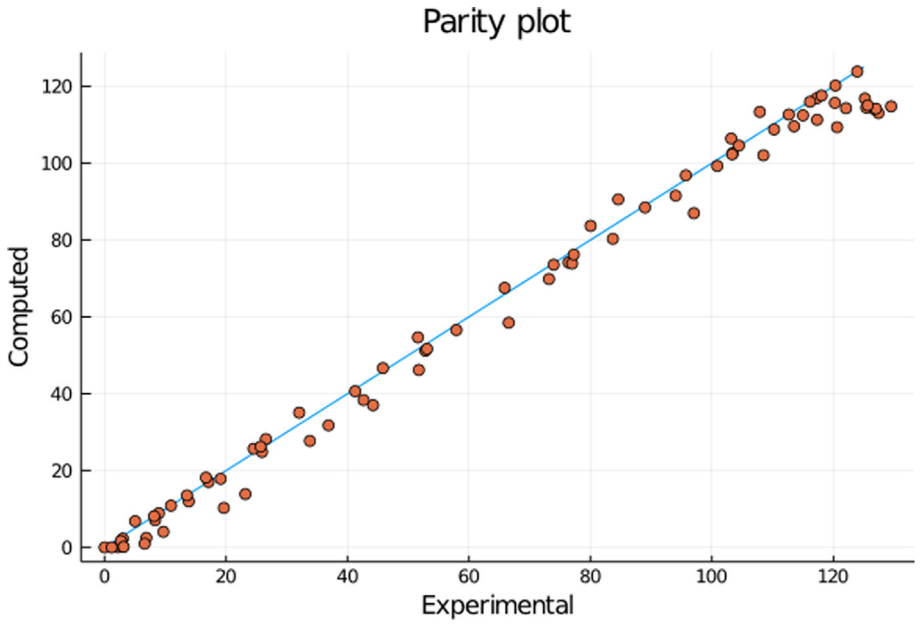

Fig. 9. Parity plot for variation of the oxygen partial pressure.

Table 7
Kinetic parameters estimated for varying of pH at standard conditions (Table 1).

Parameter	Value	Error/%
k_1	1.2546 10^4	7
k_2	7.5454 10^8	24
K_{ARA}	0.0140	36
K_{ARAL}	0.0944	26

Fixing K_O = 0.2411 as estimated in Table 6.

Correlation matrix

	k_1	k_2	K_{ARA}	K_{ARAL}
k_1	1.0	0.336	0.407	0.496
k_2	−0.195	1.0	0.667	0.952
K_{ARA}	0.407	0.667	1.0	0.661
K_{ARAL}	0.496	0.952	0.661	1.0

Units: k_1, k_2 = () mol min^{-1} kg^{-1} (mol/m^3)$^{-2}$, K_{ARA}, K_{ARAL} = () (mol/m^3)$^{-1}$.

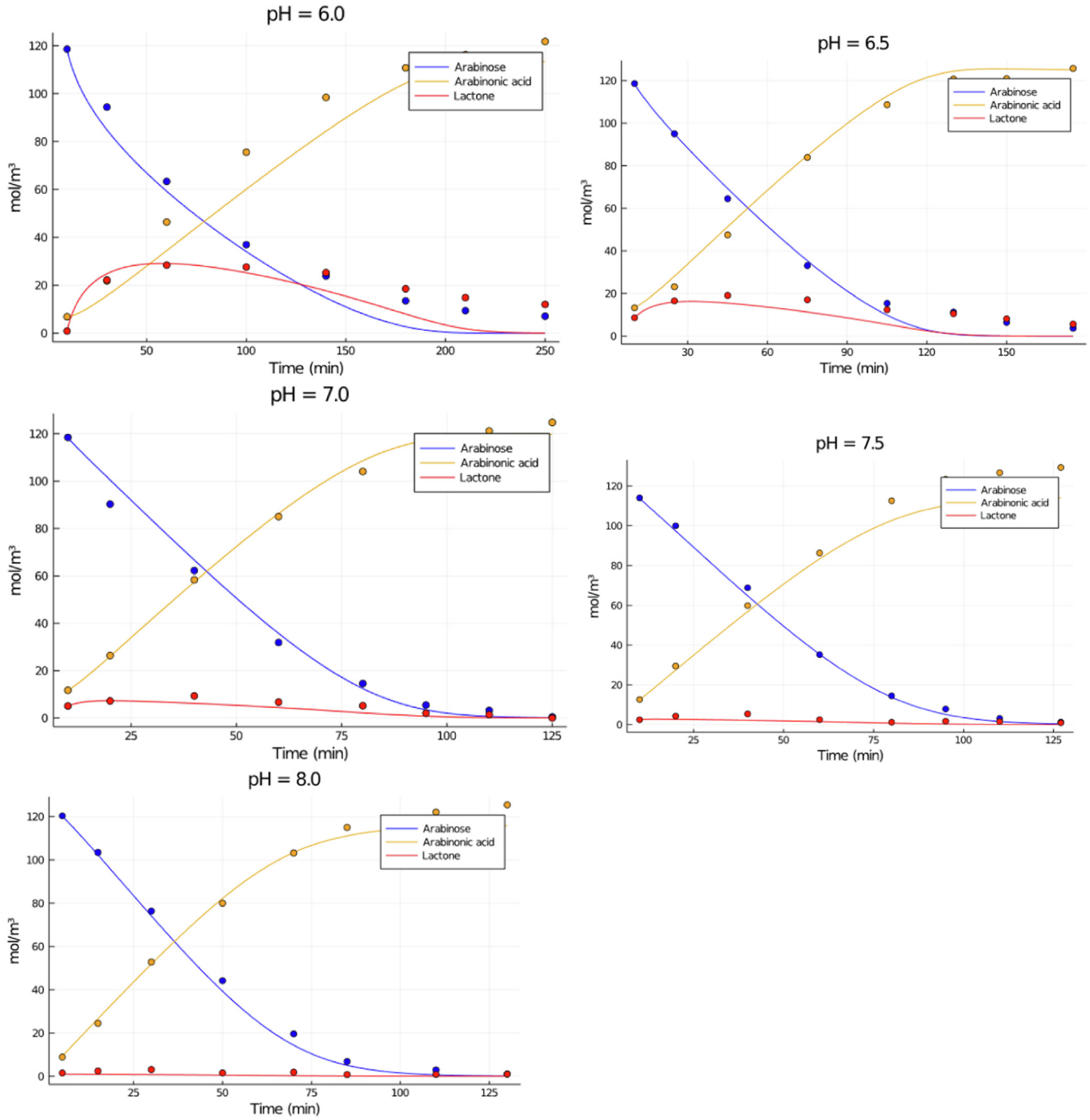

Fig. 10. Experimental (dots) and calculated (lines) concentration profiles variation of pH.

level at the partial pressure 0.125 atm. The effect of pH was investigated at the range 6–8, which gave very important results concerning the arabinolactone formation; in previous research is issue has been avoided, because lower pH (<7) favor the lactone route (Fig. 1), which is regarded as an undesirable pathway. However, to understand the kinetics more deeply, it is necessary to conduct experiments at acidic and neutral pH to observe the lactone formation and prove the consecutive mechanism of its formation and decay. The experimental results of the pH effect in Fig. 10 confirm this consecutive process for the lactone and demonstrates clearly that low pH increases the lactone formation. The concentration curves of the lactone at pH 6.0 and 6.5 enable the modelling of the lactone concentration, in a reliable way, which has not been possible in previous research (Kusema et al., 2012, Da Silva Correia et al., 2019, Herrero Manzano et al., 2021).

The kinetic constant for the second reaction is much higher than for the first one, rendering the first reaction to be rate-determining. Usually this would lead to no relevant amounts of arabinolactone in the reaction mixture as the arabinolactone produced in the reaction route N^{I} is immediately consumed by route N^{II}. Since the lactone was found in non-negligible amounts in acidic and neutral environment, other factors have to inhibit the follow-up reaction. An explanation might be the higher adsorption coefficient of arabinolactone compared to the adsorption coefficient of the arabinose. In an alkaline environment this does not really affect the reaction as the concentration of arabinose is much larger than that of

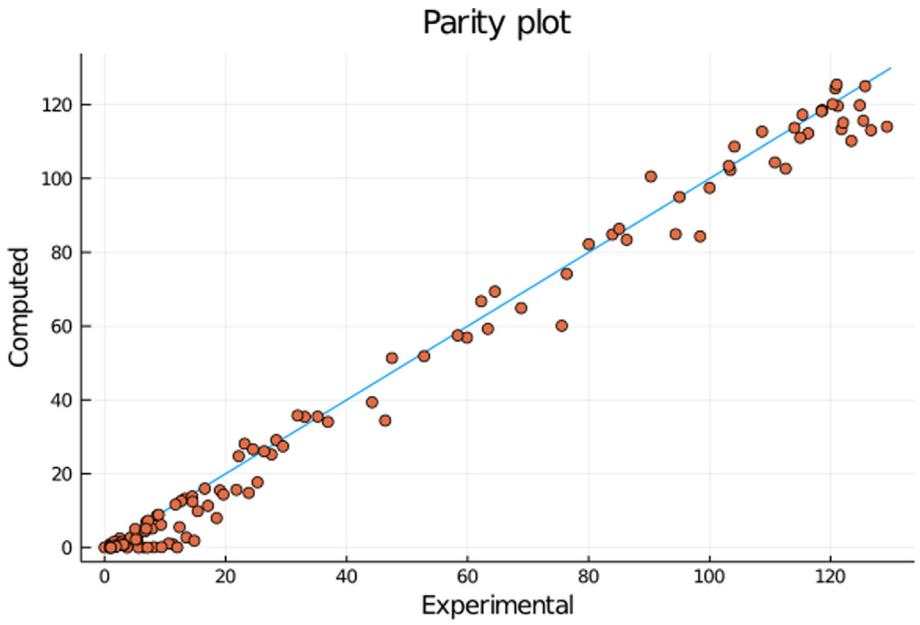

Fig. 11. Parity plot for variation of the pH.

arabinolactone. However, in acidic environment, this changes as the concentration of the arabinolactone increases strongly indicating together with the adsorption constant a high coverage of the lactone on the catalyst surface. The dependence between the adsorption of arabinolactone and the reaction rate for N^{II} is also shown by the high correlation for k_2' and K_{ARAL}. This also limits the reliability of these two parameters. However, the results suggest that the lactone acts as an inhibitor to the overall reaction in acidic environment which is in accordance with the results reported by Da Silva Correia et al. (2019). All other estimated parameters showed much lower correlations indicating a good reliability. Additionally, the parity plots considering the concentrations of all the components confirmed the good agreement of the calculated and the experimental data. Only at low concentrations, large deviations exceeding 10 % became visible. These deviations can be explained by systematic errors as the peak-splitting method used for analyzing the HPLC chromatogram is less precise at lower concentrations, especially for the determination of the arabinolactone concentration.

7. Conclusions

Finely dispersed gold catalyst particles were successfully used in the laboratory-scale slurry reactor to oxidize arabinose to arabinonic acid. The new features of this work were in the systematic investigation of the influence of oxygen partial pressure and pH on the reaction kinetics and product distribution. Extensive measurements of the oxygen solubility were carried out and these data were used in the kinetic modelling of the oxidation process in the slurry reactor. The most important result of this work was that the kinetic model which is able to describe the essential phenomena in arabinose oxidation in the parameter space, taking into account the variations of the key parameters, oxygen pressure and pH. Because of the analogous behavior of monomeric sugars, it is very probable that the proposed reaction kinetic model will find applications in the oxidation of other monomeric sugars, too.

CRediT authorship contribution statement

Bernadette Worgul: Methodology, Validation, Formal analysis, Investigation, Data curation, Writing – original draft. **Adriana Freites Aguilera:** Conceptualization, Methodology, Validation, Formal analysis, Investigation, Data curation, Writing – original draft, Writing – review & editing. **Camille Vergat-Lemercier:** Methodology, Validation, Formal analysis, Investigation, Data curation, Writing – original draft. **Kari Eränen:** Conceptualization, Methodology, Supervision, Project administration, Funding acquisition. **Olga Simakova:** Methodology, Validation, Formal analysis. **Hendrik Held:** Conceptualization, Methodology, Supervision, Project administration. **Hansjörg Freund:** Conceptualization, Methodology, Supervision, Project administration, Funding acquisition. **Dmitry Yu. Murzin:** Conceptualization, Methodology, Writing – original draft, Supervision. **Tapio Salmi:** Conceptualization, Methodology, Writing – original draft, Writing – review & editing, Supervision, Project administration, Funding acquisition.

Declaration of Competing Interest

The authors declare that they have no known competing financial interests or personal relationships that could have appeared to influence the work reported in this paper.

Acknowledgement

This research effort is a part of the activities financed by Academy of Finland, the Academy Professor grants 319002, 320115, 345053 (Tapio Salmi) and 320115 (Adriana Freites Aguilera). The economic support from Academy of Finland is gratefully acknowledged. The work is partially financed by the Erasmus Mundus student exchange programme (Bernadette Worgul, Camille Vergat-Lemercier). The authors are grateful to Dr Markus Peurla (University of Turku) for consultations of the HR-TEM measurements.

Appendix A. Supplementary material

Supplementary data to this article can be found online at https://doi.org/10.1016/j.ces.2022.117948.

References

Battino, R., 1981. *Solubility Data Series*, Vol. 7, Oxygen and Ozone. Pergamon Press. https://srdata.nist.gov/solubility/IUPAC/SDS-10/SDS-10.pdf.

Behravesh, E., Melander, M., Wärnå, J., Salmi, T., Honkala, K., Murzin, D., 2020. Oxidative dehydrogenation of ethanol on gold: Combination of kinetic experiments and computation approach to unravel the reaction mechanism. J. Catal. 394, 193–205.

Correia, L.S., Grénman, H., Wärnå, J., Salmi, T., Murzin, D.Y., 2019. Catalytic oxidation kinetics of arabinose on supported gold nanoparticles. Chem. Eng. J. 370, 952–961.

Delidovich, I.V., Moroz, B.L., Taran, O.P., Gromov, N.V., Pyrjaev, P.A., Prosvirin, I.P., Bukhtiyarov, V.I., Parmon, V.N., 2013. Aerobic selective oxidation of glucose to gluconate catalyzed by Au/Al_2O_3 and Au/C: Impact of the mass-transfer processes on the overall kinetics. Chem. Eng. J. 223, 921–931.

Dissolved Oxygen Tables, calibration and oxygen solubility tables, 2019. . YSI, a Xylem brand. https://www.ysi.com/File%20Library/Documents/Technical%20Notes/DO-Oxygen-Solubility-Table.pdf.

Fogg, P.G.T., Gerrard, W., 1991. Solubility of Gases in Liquids. Wiley, Chichester.

Franz, S., Shcherban, N.D., Simakova, I.L., Peurla, M., Eränen, K., Wärnå, J., Salmi, T., Murzin, D.Y., 2021. Oxidation of glucose and arabinose mixtures over Au/Al_2O_3. Reaction Kinet., Mech. Catal. 132 (1), 59–72.

Haruta, M., 1989. Gold catalysts prepared by co-precipitation for low-temperature oxidation of hydrogen and of carbon monoxide. J. Catal. 115 (2), 301–309.

Hashmi, A.S.K., Hutchings, G.J., 2006. Gold Catalysis. Angew. Chem. Int. Ed. 45 (47), 7896–7936.

Herrero Manzano, M., Eränen, K., Freites Aguilera, A., Wärnå, J., Franz, S., Peurla, M., García Serna, J., Murzin, D., Salmi, T., 2021. Interaction of intrinsic kinetics, catalyst durability and internal mass transfer in the oxidation of sugar mixtures on gold nanoparticle extrudates. Ind. Eng. Chem. Res., Professor Enrico Tronconi Festschrift 60 (18), 6483–6500.

Kusema, B.T., Campo, B.C., Mäki-Arvela, P., Salmi, T., Murzin, D.Y., 2010. Selective catalytic oxidation of arabinose—A comparison of gold and palladium catalysts. Appl. Catal. A 386 (1-2), 101–108.

Kusema, B.T., Hilmann, G., Mäki-Arvela, P., Willför, S., Holmbom, B., Salmi, T., Murzin, D.Y., 2011. Selective hydrolysis of arabinogalactan into arabinose and galactose over heterogeneous catalysts. Catal. Lett. 141 (3), 408–412.

Kusema, B.T., Mikkola, J.-P., Murzin, D.Y., 2012. Kinetics of L-arabinose oxidation over supported gold catalysts with in situ catalyst electrical potential measurements. Catal. Sci. Technol. 2 (2), 423–431.

Kusema, B.T., Murzin, D.Y., 2013. Catalytic oxidation of rare sugars over gold catalysts. Catal. Sci. Technol. 3 (2), 297–307.

Luterbacher, J.S., Martin Alonso, D., Dumesic, J.A., 2014. Targeted chemical upgrading of lignocellulosic biomass to platform molecules. Green Chem. 16 (12), 4816–4838.

Mehtiö, T., Toivari, M., Wiebe, M.G., Harlin, A., Penttilä, M., Koivula, A., 2016. Production and applications of carbohydrate-derived sugar acids as generic biobased chemicals. Crit. Rev. Biotechnol. 36 (5), 904–916.

Mirescu, A., Prüße, U., 2007. A new environmental friendly method for the preparation of sugar acids via catalytic oxidation on gold catalysts, 2007. Appl. Catal. B 70 (1-4), 644–652.

Murzin, D.Y., Salmi, T., 2012. Catalysis for lignocellulosic biomass processing: methodological aspects. Catal. Lett. 142 (6), 676–689.

Murzina, E.V., Tokarev, A.V., Kordás, K., Karhu, H., Mikkola, J.-P., Murzin, D.Y., 2008. D-Lactose oxidation over gold catalysts. Catal. Today 131 (1-4), 385–392.

Price, C.A.H., Pastor-Pérez, L., Ivanova, S., Reina, T.R., Liu, L., 2019. The success story of gold-based catalysts for gas- and liquid-phase reactions: A brief perspective and beyond. Front. Chem. 7, 691.

Salmi, T., Murzin, D.Y., Mäki-Arvela, P., Kusema, B., Holmbom, B., Willför, S., Wärnå, J., 2014. Kinetic modeling of hemicellulose hydrolysis in the presence of homogeneous and heterogeneous catalysts. AIChE J. 60 (3), 1066–1077.

Simakova, O., Kusema, B., Campo, B., Leino, A.R., Kordás, K., Pitchon, V., Mäki-Arvela, P., Murzin, D., 2011. Structure Sensitivity in L -Arabinose Oxidation over Au/Al_2O_3 Catalysts. J. Phys. Chem. C 115, 1036–1043.

van Stroe-Biezen, S., Janssen, A., Janssen, L., 1993. Solubility of oxygen in glucose solutions. Anal. Chim. Acta 280 (2), 217–222. https://doi.org/10.1016/0003-2670(93)85124-3.

Thompson, D.T., 2006. An overview of gold-catalysed oxidation processes. Top. Catal. 38 (4), 231–240.

Tromans, D., 1998. Temperature and pressure dependent solubility of oxygen in water: a thermodynamic analysis. Hydrometallurgy 48 (3), 327–342.

Weisenberger, S., Schumpe, A., 1996. Estimation of gas solubilities in salt solutions at temperatures from 273 K to 363 K. AIChE J. 42 (1), 298–300.

Weisz, P.B., Hicks, J.S., 1962. The behavior of porous catalyst particles in view of internal mass and diffusion effects. Chem. Eng. Sci. 17, 265–275.

White, J.M., 2020, *The LsqFit least squares fitting package*, https://github.com/uliaNLSolvers/LsqFit.jl.

Wilhelm, E., Battino, R., Wilcock, R. J., 1974. *Solubility of Gases in Water*. Chem. Rev., 77(2).